

# Bone Metabolic Activity Around Dental Implants Under Loading Observed Using Bone Scintigraphy

Hiroto Sasaki, DDS, PhD<sup>1</sup>/Shigeto Koyama, DDS, PhD<sup>2</sup>/Masayoshi Yokoyama, DDS, PhD<sup>3</sup>/  
Keiichiro Yamaguchi, MD<sup>4</sup>/Masatoshi Itoh, MD<sup>4</sup>/Keiichi Sasaki, DDS, PhD<sup>5</sup>

**Purpose:** The purpose of this study was to determine dynamic changes in bone metabolism around osseointegrated titanium implants under mechanical stress. **Materials and Methods:** Two titanium implants were inserted parallel to each other in the tibiae of rats and perpendicular to the bone surface with the superior aspect of the implant exposed. Eight weeks after insertion, closed coil springs with 0.5, 1.0, 2.0, and 4.0 N were applied to the exposed superior portion of the implant for 7 weeks to apply a continuous mechanical stress. Bone scintigrams were performed using a gamma camera with a modified high-resolution pinhole collimator. Images were made at 1, 4, 7, 10, 14, 21, 28, 49, and 56 days after insertion and at 3 days and at weekly intervals until 7 weeks after load application. The ratio of the metabolic activity around the implants to that around a reference site (uptake ratio) was established. The Friedman, Steel, and Tukey tests ( $P < .05$ ) were used to assess statistical significance. **Results:** In the process of osseointegration, the uptake ratio increased during the first week after implant insertion and then gradually decreased. During the initial 3 weeks the uptake ratio was significantly higher than at 1 day after insertion. In the process of load application, the uptake ratio increased with 2.0- and 4.0-N loads; it was significantly higher until 6 weeks than it had been before load application. **Conclusions:** Bone metabolism around the implants increases with loading and depends on the magnitude and period of the loading. INT J ORAL MAXILLOFAC IMPLANTS 2008;23: 827-834

**Key words:** bone metabolism, bone remodeling, bone scintigraphy, mechanical stress, osseointegrated titanium implant

A load-bearing dental implant transmits occlusal forces to the adjacent bone directly. While the load on the dental implant is considered a determinant of the success of the implant in the long term, there is little evidence supporting this theory. A few studies have suggested that occlusal overload may

contribute to implant bone loss and/or loss of integration of successfully integrated implants.<sup>1-5</sup> Isidor<sup>2,3</sup> reported implant mobility caused by progressive peri-implant bone loss after the implant was exposed to mechanical occlusal trauma for 18 months. On the other hand, others believe that peri-implant bone loss and/or disintegration are associated with biologic complications such as peri-implant infection.<sup>6,7</sup>

Therefore, whether occlusal overload is a causative or contributing factor in late implant failures continues to be a point of discussion.<sup>8,9</sup> From the standpoint of biologic effects on the bone-implant interface, it is possible that osseointegration depends on implant loading.<sup>10</sup> In particular, excessive occlusal loading might lead to disintegration, while adequate loading might lead to adaptive remodeling of the bone around the implant.<sup>8,9</sup>

There is general agreement that a certain level of mechanical loading is required for normal bone remodeling.<sup>10</sup> Osseointegration generally follows 3

<sup>1</sup>Assistant Professor, Division of Advanced Prosthetic Dentistry, Tohoku University Graduate School of Dentistry, Sendai, Japan.

<sup>2</sup>Associate Professor, Maxillofacial Prosthetics Clinic, Tohoku University Hospital, Sendai, Japan.

<sup>3</sup>Visiting Professor, Division of Dental Pharmacology, Tohoku University Graduate School of Dentistry, Sendai, Japan.

<sup>4</sup>Professor Emeritus, Tohoku University Cyclotron Radioisotope Center, Sendai, Japan.

<sup>5</sup>Professor, Division of Advanced Prosthetic Dentistry, Tohoku University Graduate School of Dentistry, Sendai, Japan.

**Correspondence to:** Dr Shigeto Koyama, Maxillofacial Prosthetics Clinic, Tohoku University Hospital, 4-1, Seiryomachi, Aoba-ku, Sendai, Miyagi, 980-8575, Japan. Fax: +81 22 717 8371. E-mail: koyama@mail.tains.tohoku.ac.jp

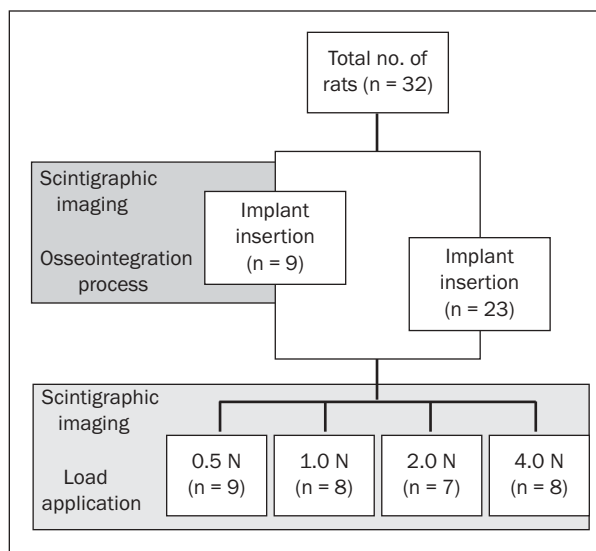


**Fig 1** Flowchart of the experiment.

stages: (1) incorporation by woven bone formation, (2) adaptation of bone mass to load (lamellar and parallel-fibered deposition), and (3) adaptation of bone structure to load (bone remodeling).<sup>11</sup> During the third stage, when functional loading has been initiated, the bony structures adapt to the load by improving the quality of the bone, replacing pre-existing, necrotic and/or initially formed more primitive woven bone with mature, viable lamellar bone. This leads to functional adaptation of the bony structures to the load—the dimensions and orientation of the supporting elements change. Misch<sup>12</sup> claimed that the change in bone strength from loading and mineralization after 1 year alters the stress-strain relationship and reduces the risk of microfracture during the following year.

Mechanical stress thus might induce a metabolic turnover of the bone based on the changes in osteocyte responses around the implant, resulting in bone remodeling. However, few studies have been conducted on bone remodeling and adaptation under continuous loading of an osseointegrated oral implant.

Regarding bone metabolic activity, such as bone remodeling and adaptation, histologic studies can merely depict static and cross-sectional aspects of the bone activity and phenomena in the remodeling process. In contrast, a nuclear medicine approach with radionuclide bone scanning, including scintigraphy, is widely used to evaluate the dynamic and longitudinal processes in biologic response. A common preparation is Tc99m-methylene diphosphonate (Tc99m-MDP). In vivo scintigraphic imaging using Tc99m-MDP enables the same region to be observed

numerous times without sacrificing the host animal. Studies can thus be done over time, and multiple within-subject comparisons can be obtained. In short, bone scanning using scintigraphy provides a dynamic determination of the metabolic activity around the implant.

The aim of this study was to investigate the dynamic changes in bone metabolism around osseointegrated implants under mechanical stress. This was done using bone scintigraphy and Tc99m-MDP.

## MATERIALS AND METHODS

### Animals and Insertion of Implants

The guidelines for animal use (NIH Animal Research Advisory Committee, 1995) as well as specific national laws were followed. The preparation was performed according to animal protocols approved by Tohoku University. Thirty-two 12-week-old male Wistar rats were used. Nine rats were used to investigate the biologic process of osseointegration after implant insertion, and 23 rats were used to investigate the bone metabolic activity under loading (Fig 1). The rats were anesthetized with sodium pentobarbital (50 mg/kg) administered intraperitoneally with supplemental ether inhalation. An incision was made in the medial aspect of the tibia, and an osteotomy was performed using a surgical drill with irrigation. According to a 1-stage surgical protocol, 2 titanium implants (Orthoanchor; Dentsply-Sankin, Tokyo, Japan) 1.2 mm in diameter and 9.25 mm in length (Fig 2), were placed in the tibiae perpendicular to the bone surface; the implant heads were exposed about 5 mm (Fig 3). In each rat, 1 implant was placed 10 mm from the knee joint. The other was placed 13 mm distal from the first. The experiments were carried out under aseptic conditions.

### Loading with Coil Springs

Healing and osseointegration were in progress at 8 weeks after insertion. To clarify the biologic responses around the implants under continuous loading, closed coil springs (Sentalloy; Tomy International, Oookuma, Japan) were attached to the implant heads of 9 rats for 7 weeks to apply a continuous mechanical stress (0.5 N; Fig 4a). Closed coil springs with 1.0, 2.0, or 4.0 N were also attached to the implant heads of 8, 7, and 8 rats, respectively. The group of rats with two 2.0-N springs was defined as the 4.0-N loading group (Fig 4b). Each spring was 10 mm long and made of nickel-titanium alloy. It comprised a tension coil (3 mm long) and a hook attachment (7 mm long). The effective length of the tension coil was 12 mm (3 to 15 mm tension coil length). The

**Fig 2** Implant body. Photograph shows commercially pure titanium implant for orthodontic anchorage. Entire length of implant was 9.25 mm, and its diameter was 1.2 mm.

**Fig 3** Lateral view of right pelvic limb. Two implants were placed perpendicular to long axis of tibia at an interval of 13 mm with implant heads exposed for attaching coil springs.

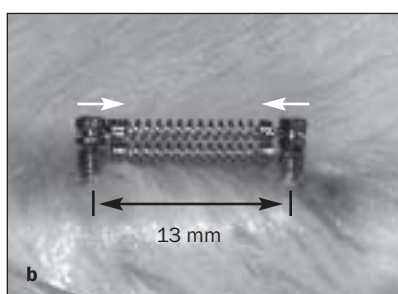
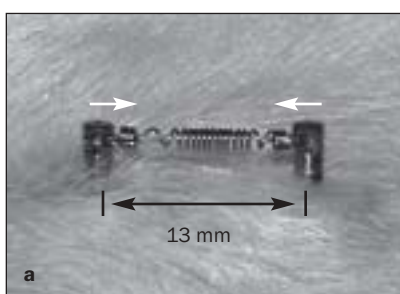
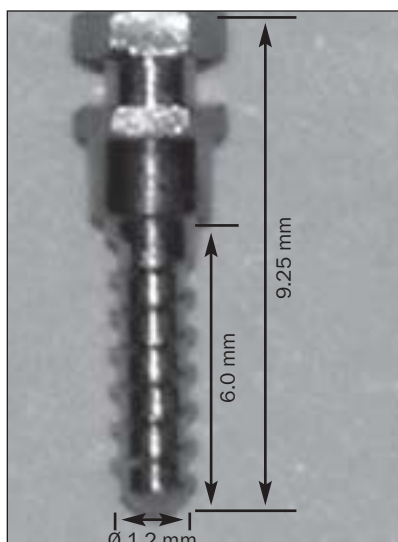


**Fig 4** Attached closed coil springs. Eight weeks after implant insertion, closed coil springs were attached to implant heads. (a) With loading of 0.5, 1.0, or 2.0 N, closed coil springs were set prospectively. (b) Two closed coil springs with loading of 2.0 N each were set in parallel for total loading of 4.0 N. Arrows show loading directions.

**Fig 5** Set-up for image taking. Photograph shows rat on exclusive table in dorsal position with implant heads in a vertical position. Device fixes tibia horizontally to equalize distance of implants from pinhole collimator. Image taking was carried out from the backside of rat with scintillator and modified pinhole collimator.

hook attachment was modified to hook onto the implant heads. The springs thus applied the same magnitude of loading continuously within their effective length (10 to 22 mm).

### Scintigraphic Imaging

To observe the bone metabolic activity around the implants *in vivo*, scintigraphic images of the bone were obtained using a gamma camera (ZLC7500, Siemens, Munich, Germany) with a modified high-resolution pinhole collimator 2 mm in diameter. The collimator was fabricated from lead with a smaller diameter to enable imaging of small regions, such as the bone around the implants. Tc-99m-MDP was used as a radioisotope tracer. Sodium pertechnetate (Na<sup>99m</sup>Tc-O<sub>4</sub>) was eluted from a generator (Ultra-Techne Kow, Daiichi Radioisotope Laboratories, Chiba, Japan) and mixed with methylene diphosphate (Techne MDP injection solution, Daiichi

Radioisotope Laboratories, Chiba, Japan) at room temperature. Five minutes after this mixing, the Tc<sup>99m</sup>-MDP was injected into a vein of the tail of each rat (74 MBq/rat). Static-planar acquisition was initiated 2 hours after the injection and finished at 50,000 counts with a 512 × 512 matrix size. The rats were fixed on an exclusive table in the dorsal position, with the implant heads turned to a vertical position. A device was used to fix the tibia horizontally to equalize the distance of the implants from the collimator. The images were taken from the backside direction of the rat (Fig 5).

To clarify the bone metabolic activity around the implants during osseointegration, images were taken at 1, 4, 7, and 10 days and 2, 3, 4, 7, and 8 weeks postimplantation. To clarify the bone metabolic activity around the implants under continuous loading, images were taken at 3 and 7 days and 2, 3, 4, 5, 6, and 7 weeks after loading with the coil springs.

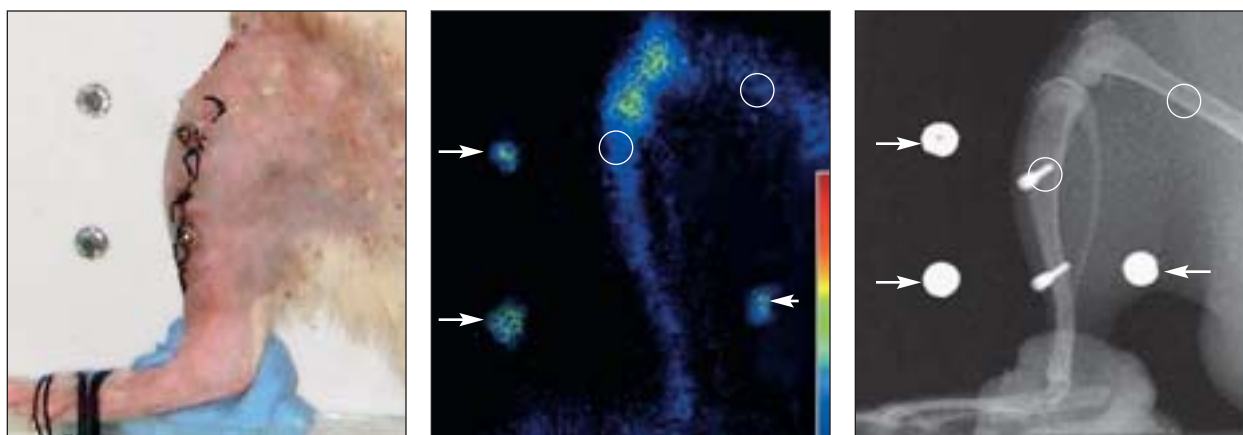


**Fig 6** Image analysis. Photograph on the left shows tibia fixation on the exclusive table. Device fixed tibia horizontally to equalize the distance of implants from the pinhole collimator. Scintigram in the center and radiographic image on the right show planar images. Guide tubes (arrows) were used to overlap 3 images and to define the region of interest (open circles).

### Radiographic Imaging

To identify the region of the reference site (middle part of femur) and the implants, a radiograph was obtained of each rat on the table using an imaging plate (IP; BAS-SR2505, Fuji Film, Tokyo, Japan), with an x-ray tube voltage of 70 kV and a tube current-time product of 9 mA. Each imaging plate was then scanned with an imaging analyzer (BAS5000, Fuji Film, Tokyo, Japan) and translated for use in a personal computer. The exclusive table had 3 markers (lead) and acrylic tubes 0.9 mm in diameter. Before the scintigraphic imaging, Tc99m-MDP (about 0.37 MBq) was placed in each tube, resulting in an accumulation of Tc99m-MDP in the tube regions on the scintigrams for each rat. These markers indicate the points of overlap with the lead regions in the radiographic images, enabling identification of the implant and reference sites (Fig 6).

### Data Processing

The scintigrams were translated into TIFF format (16 bits) with a data processing unit (Scintipac 700, Shimazu, Japan) and conversion software (picMAO, Shimazu, Kyoto, Japan). After they were transferred to a personal computer (Macintosh LC475, Apple, Cupertino, CA), analysis processing was conducted with image analysis software (Osiris, Geneva University Hospital, Geneva, Switzerland).

### Accumulation Measurement

After identification of the implant and reference sites by the overlapping of the radiographic images and scintigrams, a round region of interest (161 pixels) was defined around both sites, and the accumula-

tions of Tc99m-MDP in both regions were measured. The ratio of the metabolic activity around the implants to that around the reference site (uptake ratio) was calculated.

### Statistical Analysis

The collected data were analyzed using Friedman, Steel, and Tukey tests with statistical software (SPSS 11.0; SPSS, Chicago, IL).  $P$  values  $< .05$  were deemed statistically significant.

## RESULTS

No clinical mobility of the implants was observed for the entire experimental period.

### Metabolic Changes After Insertion of Implants

The uptake ratio increased during the first week after implant insertion and then decreased gradually. It was significantly higher than baseline on days 4, 7, and 10 ( $P < .01$ ; Friedman test) and during the second and third weeks ( $P < .05$ , Steel test). However, it was not significantly higher at 4 weeks and 7 weeks (ie, metabolic activity had returned to the baseline level; Fig 7).

### Metabolic Changes After Loading

*Effect of Loading Period.* The uptake ratio changed with the loading. With 2.0- and 4.0-N loading, change of activities over the 7-week experimental period were almost the same in terms of magnitude and timing. The ratio reached a maximum during the first week (more than twice that without loading) and

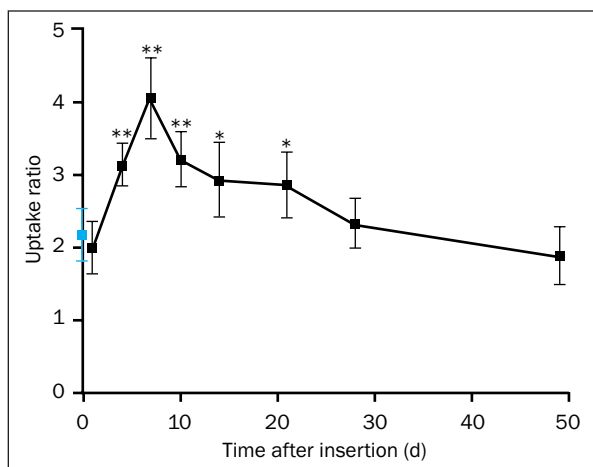


**Fig 7** Change in uptake ratio after insertion of implants using 9 rats. There were significant differences at days 4, 7, and 10 and in the second and third weeks after insertion. Blue = control. \* $P < .05$ , \*\* $P \leq .001$ .

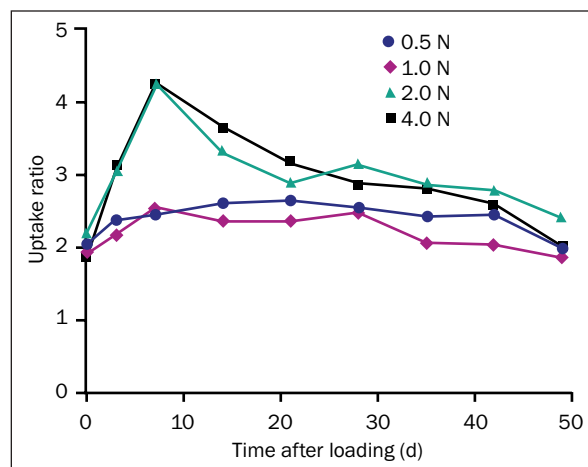


**Fig 8** Change in uptake ratio after loading with coil springs using 32 rats. There were significant differences between 2.0- and 4.0-N load and the 0.5- and 1.0-N. With 2.0- and 4.0-N loading, the ratio from 3 days to 6 weeks after loading was significantly higher than that without loading.

then decreased a little. Metabolic activity returned to the baseline level. The ratio then returned to baseline level at about 2 to 7 weeks after loading. The ratio from 3 days to 6 weeks after loading was significantly higher than without loading (Friedman and Steel tests,  $P < .05$ ). There was no significant difference 7 weeks after loading.

The results for the 0.5- and 1.0-N loading groups were similar but differed from those for the 2.0- and 4.0-N loading groups. With the smaller loadings, the uptake ratio gradually increased after loading and returned to the baseline level at 7 days. It then decreased, reaching baseline level at 2 to 7 weeks after loading. With 1.0-N loading, the uptake ratio did not differ among measurement points (Friedman and Steel tests,  $P > .05$ ).

**Effect of Loading Magnitude.** The uptake ratios with the 2.0- and 4.0-N loads were significantly higher than those with the 0.5- and 1.0-N loads (Tukey test,  $P < .05$ ; Fig 8).

## DISCUSSION

Osseointegration is defined as direct bone deposition on implant surfaces at the light-microscopic level.<sup>13</sup> In vitro studies have illustrated the importance of loading forces on the nature of the interface between an implant and the surrounding tissues.<sup>14,15</sup> Even if implants are initially integrated, the application of excessive loading can create microfractures and relative motion, which can promote bone resorption in the immediate vicinity of the implant and repair by growth of fibrous tissue.<sup>16,17</sup> However,

changes, including bone turnover around implants due to mechanical stress, have not been fully elucidated. Thus, the biologic mechanism of bone metabolism around implants must be clarified.

Therefore, the nuclear medicine approach using radionuclide bone scans (eg, scintigraphy, single-photon emission computerized tomography [SPECT], positron emission tomography [PET]) has been used to investigate bone metabolism. This approach enables the dynamic and longitudinal processes in biologic responses to be evaluated. It is widely used clinically with radiopharmaceutical isotopes to detect tumors of osteogenic origin and to help in comprehending the condition of osseointegration.<sup>18-21</sup>

This study was conducted using bone scintigraphy and Tc99m-MDP. The specific binding location of Tc99m-MDP remains unknown, although it is associated with areas of bone growth and osteoblast activity.<sup>22-25</sup> Areas with an observed accumulation of radiopharmaceutical isotopes showed an increased level of bone metabolic activity, suggesting that this method enables measurement of the changes in bone metabolic activity around implants in vivo.<sup>26-29</sup> Furthermore, bone scintigraphy makes it possible to observe the accumulations with more sensitivity and higher reactivity over time than with conventional radiology.<sup>30</sup> Moreover, it is not invasive, as are histologic methods. Therefore, this method is suitable for the longitudinal observation of bone metabolic activity.

Generally, a pinhole collimator with a diameter of more than 6 mm is used when targeting human internal organs. However, its resolution is too low for small regions, such as the bone around an implant in rats. The resolution and sensitivity of a pinhole colli-

mator depend on the diameter of the pinhole and on the distance to the object.<sup>31</sup> The smaller the diameter, the higher the resolution, but sensitivity is degraded, which lengthens the imaging time. Furthermore, the closer the collimator is to the object, the higher the sensitivity, but the field of view becomes narrower. In this study, a pinhole collimator made of lead with a diameter of 2 mm was fabricated, and the distance from the collimator to the target was set at 20 mm to achieve the best balance among resolution, sensitivity, and field of view.

### Process of Osseointegration

Regarding the osseointegration process, a histologic study of implant insertion in the rat tibia by Masuda et al<sup>32</sup> showed that the forming matrix was clearly consolidated 28 days after insertion. Other histologic studies using rat tibia have shown similar results.<sup>33–35</sup> Based on the results of morphologic and radioautographic studies, Clokie et al<sup>36,37</sup> asserted that osseointegration is completed 6 weeks after insertion of an implant in the rat tibia.

In the present study, the metabolic activity around the implants increased through the first week and then gradually decreased. There was no significant difference between the activity on day 1 and at week 4. Additionally, no clinical mobility of the implants was observed during the healing period. These results and those of previous studies suggest that osseointegration is obtained about 4 weeks after implant insertion. Thus, in this study, loading using closed coil springs was applied to the implant heads 8 weeks after implantation to have a sufficient margin. In addition, the timing of the peak level of and subsequent decrease in bone metabolic activity found in this study correspond very well to those of a previous report on Tc99m-MDP activity around implants using bone scintigraphy.<sup>20</sup> Therefore, it should be possible to observe in real time the osseointegration process and the degrees and stages of bone metabolism using this method longitudinally.

### Changes in Bone Metabolic Activity Due to Loading

In the present investigation, the heavy loading (2.0 and 4.0 N) group showed a remarkable increase in the uptake ratio compared with the light loading (0.5 and 1.0 N) group. This indicates that the metabolic activities are affected by the magnitude of the mechanical loading on the implant. In a histologic study, Hoshaw et al<sup>38</sup> reported a decreased percentage of mineralized bone tissue in a 350- $\mu$ m-wide zone around implants following axial loading with a triangular waveform for 500 cycles per day for 5 consecutive days. In contrast, Gotfredsen et al<sup>39–42</sup>

demonstrated that implants subjected to a static lateral expansion load showed increased bone density and mineralized bone-implant contact compared with control implants. Melsen and Lang<sup>43</sup> reported that there was significantly higher bone apposition around loaded implants than unloaded implants, but the dimensions of the applied load did not affect the turnover characteristics of the peri-implant alveolar bone. These results suggest that bone metabolic activity is changed by mechanical stress and that it depends on the loading conditions, such as the direction, quality, and duration of the loading.

In the present study, the uptake ratio showed dynamic changes, and the peak levels were similar in the heavy loading group (ie, there was no difference between 2.0- and 4.0-N loading). It is conceivable that the bone metabolic activity may have an upper limit, the point where the loading exceeds the physiologic threshold of bone adaptation.<sup>44</sup> On the other hand, it is possible that the bone metabolic activity increases remarkably when excessive loading is applied to the implant, causing implant disintegration.

Miyata et al<sup>4</sup> described occlusal overload employed with 3 different excess occlusal heights (100  $\mu$ m, 180  $\mu$ m, 250  $\mu$ m) on implant prostheses for 4 weeks. Bone destruction was observed in the 180- $\mu$ m and 250- $\mu$ m excess occlusal height groups, and there was evidence of the existence of a critical point of excessive occlusal height on the prostheses for crestal bone loss.

However, in this study, we were unable to define a "normal physiologic range" for the loading applied to osseointegrated implants. Future studies are needed to elucidate the role of mechanical stress in osseointegration.

### Bone Adaptation to Mechanical Stress

In the present study, it was found that the bone metabolic activity gradually decreased from the peak level. Despite the application of a static force to the implants, it eventually returned to the preloading level. This change can be attributed to an adaptive bone remodeling process similar to those previously reported. Saxon et al<sup>45</sup> demonstrated that mechanical loading on the rat ulna greatly improved bone formation during the first 5 weeks of loading, while continual loading reduced the osteogenic response. Moreover, restoring the same level of loading after a period of no loading increased bone formation again. Warden et al<sup>46</sup> investigated the use of mechanical loading with the rat ulna to induce bone adaptation and found that fatigue resistance was more advanced in bone loading than a control group because the structural properties changed due to loading. Loading is thus an important factor in the

formation and maintenance of skeletal architecture. Bone morphology adapts to the functional loading patterns by responding to the size and distribution of strains that loading engenders in the bone tissue.<sup>47,48</sup> It is concluded that in the present study the bone around the implants adapted to the mechanical stress of long-term loading by structurally changing and that the responsiveness to the loading diminished over time. Furthermore, functional adaptation and maintenance of the bony structures around implants may be caused by cells (ie, osteocytes, osteoblasts, or osteoclasts) in active response to environmental biophysical stimuli; in other words, mechanical stress.

Microstrain levels 100 times less than the ultimate strength of bone may be responsible for remodeling rates within the structure, since the bone cell membranes are able to act as a mechanosensory system in bone.<sup>49</sup> The cellular behavior of bone cells is largely determined by the mechanical environment of strain or deformation of the bone cell.<sup>50</sup>

Verborgt et al<sup>51</sup> found that fatigue loading produced a large number of osteocytes in bone surrounding microcracks and stated that there was a strong association between microdamages, osteocyte apoptosis, and subsequent bone remodeling.

Noble et al<sup>52</sup> showed that mechanical loading of the bone can be used to regulate osteocyte apoptosis, which has a mechanism for the precise targeting of osteoclasts for bone adaptation. Miyata et al<sup>53</sup> speculated that long-term occlusal stress on implants within the physiologic tolerance might stimulate blood circulation, which has an intraosseous bone-inducing factor that promotes bone metabolism and, consequently, enhances bone remodeling to obtain the width needed to counter occlusal stress. However, the details are not apparent. Additional research is needed to clarify the effect of the other loading conditions in order to determine the appropriate range of force on implants. Furthermore, the cytological responses to mechanical stress are unclear and warrant examination.

## CONCLUSIONS

1. Following implant insertion, bone metabolic activity initially increased and then decreased gradually to the baseline level once osseointegration was completed.
2. Bone metabolic activity was enhanced by mechanical loading of the bone through the implant.
3. Although the same level of loading was maintained, the metabolic activity decreased over time.

## ACKNOWLEDGMENT

This work was supported by grants-in-aid for scientific research (grant no. 14370626) from the Ministry of Education, Science, and Culture of Japan.

## REFERENCES

1. Rangert B, Krogh PH, Langer B, Van Roekel N. Bending overload and implant fracture: A retrospective clinical analysis. *Int J Oral Maxillofac Implants* 1995;10:326–334.
2. Isidor F. Mobility assessment with the Periostest system in relation to histologic findings of oral implants. *Int J Oral Maxillofac Implants* 1998;13:377–383.
3. Isidor F. Histological evaluation of peri-implant bone at implants subjected to occlusal overload or plaque accumulation. *Clin Oral Implants Res* 1997;8:1–9.
4. Miyata T, Kobayashi Y, Araki H, Ohto T, Shin K. The influence of controlled occlusal overload on peri-implant tissue. Part 3: A histologic study in monkeys. *Int J Oral Maxillofac Implants* 2000;15:425–431.
5. Piattelli A, Scarano A, Favero L, Lezzi G, Petrone G, Favero GA. Clinical and histologic aspects of dental implants removed due to mobility. *J Periodontol* 2003;74:385–390.
6. Tonetti M, Schmid J. Pathogenesis of implants failures. *Periodontol* 2000 1994;4:127–138.
7. Lang NP, Wilson TG, Corbet EF. Biological complications with dental implants: Their prevention, diagnosis and treatment. *Clin Oral Implants Res* 2000;8(suppl):146–155.
8. Sanz M, Alandex J, Lazaro P, Calvo JL, Quirynen M, van Steenberghe D. Histopathologic characteristics of peri-implant soft tissues in Brånemark implants with 2 distinct clinical and radiological patterns. *Clin Oral Implants Res* 1991;2:128–134.
9. Quirynen M, Naert I, van Steenberghe D. Fixture design and overload influence marginal bone loss and fixture success in the Brånemark system. *Clin Oral Implants Res* 1992;3:104–111.
10. Frost HM. Mechanical adaptation. Frost's mechanostat theory. In: Martin RB, Burr DB (eds). *Structure, Function and Adaption of Compact Bone*. New York: Raven Press, 1989:179–181.
11. Schenk RK, Buser D. Osseointegration: A reality. *Periodontol* 2000 1998;17:22–35.
12. Misch CE. Dental evaluation: Factors of stress. In Misch CE (ed). *Contemporary Implant Dentistry*, ed 2. St Louis, MO: Mosby, 1999:122–123.
13. Brånemark P-I, Hansson BO, Adell R, et al. Osseointegrated implants in the treatment of the edentulous jaw. Experience from a 10-year period. *Scand J Plast Reconstr Surg* 1977(suppl); 16:1–132.
14. Brunski JB. Biomaterials and biomechanics in dental implant design. *Int J Oral Maxillofac Implants* 1988;3:85–97.
15. Johansson C, Albrektsson T. Integration of screw implants in rabbit: A 1-year follow-up of removal torque of titanium implants. *Int J Oral Maxillofac Implants* 1987;2:69–75.
16. Uthoff H, Germain JB. Reversal of tissue differentiation around screws. *Clin Orthopaedic Res* 1977;123:248–252.
17. Roberts WE, Garetto LP, De Castro RA. Remodeling of devitalized bone threatens periosteal margin integrity of endosseous titanium implants with treated or smooth surfaces: Indications for provisional loading and axillary directed occlusion. *J Indiana Dent Assoc* 1989;68:19–24.

18. Khan O, Archibald A, Thomson E, Maharaj P. The role of quantitative single photon emission computerized tomography (SPECT) in the osseous integration process of dental implants. *Oral Surg Oral Med Oral Pathol Oral Radiol Endod* 2000;90:228–232.
19. Shigematsu M, Shomi S, Iwao H, Ochi H. New bone-seeking agent: Animal study of Tc-99m-incadronate. *Ann Nucl Med* 2002;16:55–59.
20. McCracken M, Zinn K, Lemons JE, Thompson JA, Feldman D. Radioimaging of implants in rats using Tc-99m-MDP. *Clin Oral Implants Res* 2001;12:372–378.
21. Bambini F, Meme L, Procaccini M, Rossi B, Lo Muzio L. Bone scintigraphy and SPECT in the evaluation of the osseointegrative response to immediate prosthetic loading of endosseous implants: A pilot study. *Int J Oral Maxillofac Implants* 2004;19:80–86.
22. Kanishi D. 99mTc-MDP accumulation mechanisms in bone. *Oral Surg Oral Med Oral Pathol* 1993;75:239–246.
23. Lysell L, Rohlin M. Initial Tc-99m diphosphonate uptake in mineralized and demineralized bone implants in rats. *Int J Oral Surg* 1985;14:371–375.
24. Schwartz Z, Shani J, Soskolne WA, Touma H, Amir D, Sela J. Uptake and biodistribution of technetium-99m-MD32P during rat tibial bone repair. *J Nucl Med* 1993;34:104–108.
25. Okamoto YM. Mechanism of accumulation of 99mTc-MDP to bone: Correlation of in vivo data with in vitro data. *Radiat Med* 1997;209–215.
26. Fogelman I. Skeletal uptake of diphosphonate: A review. *Eur J Nucl Med* 1980;5:473–476.
27. Hyldstrup L, Clemmensen I, Jensen BA, Transbol I. Non-invasive evaluation of bone formation: Measurements of serum alkaline phosphatase, whole body retention of diphosphonate and serum osteocalcin in metabolic bone disorders and thyroid disease. *Scand J Clin Lab Invest* 1984;48:611–619.
28. Fleisch H. Bisphosphonates: Mechanisms of action. *Endocr Rev* 1998;19:80–100.
29. Chisin R, Gazit D, Ulmanský M, Laron A, Atlan H, Sela J. 99mTc-MDP uptake and histological changes during rat bone marrow regeneration. *Int J Rad Appl Instrum B* 1988;15:469–476.
30. Bijvoet OLM, Fleisch HA, Canfield RE, Russel RGG. Bisphosphonate on Bones. Amsterdam, Netherlands: Elsevier, 1995:87–107.
31. Weber D, Ivanovic M, Franceschi D, et al. Pinhole SPECT: An approach to in vivo high resolution SPECT imaging in small laboratory animals. *J Nucl Med* 1994;35:342–348.
32. Masuda T, Salvi GE, Offenbacher S, Felton DA, Cooper LF. Cell and matrix reactions at titanium implants in surgically prepared rat tibiae. *Int J Oral Maxillofac Implants* 1997;12:472–485.
33. Medard C, Ribaux C, Chavrier C. A histological investigation on early tissue response to titanium implants in a rat intramedullary model. *J Oral Implantol* 2000;26:238–243.
34. Guglielmotti MB, Renou S, Cabrini RL. Evaluation of bone tissue on metallic implants by energy-dispersive x-ray analysis: An experimental study. *Implant Dent* 1999;8:303–309.
35. Kajiwaru H, Yamaza T, Yoshinari M, et al. The bisphosphonate pamidronate on the surface of titanium stimulates bone formation around tibial implants in rats. *Biomaterials* 2005;26:581–587.
36. Clokie CM, Warshawsky H. Development of a rat tibia model for morphological studies of the interface between bone and a titanium implant. *Compendium* 1995;16:56–68.
37. Clokie CM, Warshawsky H. Morphologic and radioautographic studies of bone formation in relation to titanium implants using the rat tibia as a model. *Int J Oral Maxillofac Implants* 1995;10:155–165.
38. Hoshaw SJ, Brunski JB, Cochran GVB. Mechanical loading of Brånemark implants affects interfacial bone modeling and remodeling. *Int J Oral Maxillofac Implants* 1994;9:345–360.
39. Gotfredsen K, Berglundh T, Lindhe J. Bone reactions adjacent to titanium implants subjected to static load. A study in the dog (I). *Clin Oral Implant Res* 2001;12:1–8.
40. Gotfredsen K, Berglundh T, Lindhe J. Bone reactions adjacent to titanium implants with different surface characteristics subjected to static load. A study in the dog (II). *Clin Oral Implants Res* 2001;12:196–201.
41. Gotfredsen K, Berglundh T, Lindhe J. Bone reactions adjacent to titanium implants subjected to static load of different duration. A study in the dog (III). *Clin Oral Implants Res* 2001;12:552–558.
42. Gotfredsen K, Berglundh T, Lindhe J. Bone reactions at implants subjected to experimental peri-implantitis and static load. A study in the dog. *J Clin Periodontol* 2002;29:144–151.
43. Melsen B, Lang NP. Biological reactions of alveolar bone to orthodontic loading of oral implants. *Clin Oral Implants Res* 2001;12:144–152.
44. Frost HM. Wolff's Law and bone's structural adaptations to mechanical usage: An overview for clinicians. *Angle Orthod* 1994;64:175–188.
45. Saxon LK, Robling AG, Alam I, Turner CH. Mechanosensitivity of the rat skeleton decreases after a long period of loading, but is improved with time off. *Bone* 2005;36:454–464.
46. Warden SJ, Hurst JA, Sanders MS, Turner CH, Burr DB, Li J. Bone adaptation to a mechanical loading program significantly increases skeletal fatigue resistance. *J Bone Miner Res* 2005;20:809–816.
47. Lanyon LE. Control of bone architecture by functional load bearing. *J Bone Miner Res* 1992;7:369–375.
48. Lanyon LE. Functional strain in bone tissue as an objective, and controlling stimulus for adaptive bone remodeling. *J Biomech* 1987;20:1083–1093.
49. Cowin SC, Moss-Salentyin L. Candidates for mechanosensory system in bone. *J Biomech Eng* 1991;113:191–197.
50. Jones DB, Nolte H, Scholubbers JG, Turner E, Veltel D. Biochemical signal transduction of mechanical strain in osteoblast-like cells. *Biomaterials* 1991;12:101–110.
51. Verborgt O, Gibson GJ, Schaffler MB. Loss of osteocyte integrity in association with microdamage and bone remodeling after fatigue in vivo. *J Bone Miner Res* 2000;15:60–67.
52. Noble BS, Peet N, Stevens HY, et al. Mechanical loading: Biphasic osteocyte survival and targeting of osteoclasts for bone destruction in rat cortical bone. *Am J Physiol Cell Physiol* 2003;284:934–943.
53. Miyata T, Kobayashi Y, Araki H, Motomura Y, Shin K. The influence of controlled occlusal overload on peri-implant tissue: A histologic study in monkeys. *Int J Oral Maxillofac Implants* 1998;13:677–683.